Structural, electronic, and magnetic properties of Co-doped ZnO*

Bakhtiar Ul Haq[a)b)], A. Afaq[a)], R. Ahmed[b)†], and S. Naseem[a)]

[a)] *Center of Excellence in Solid State Physics, University of the Punjab, Quid-e-Azam Campus, Lahore-54590, Pakistan*
[b)] *Department of Physics, Faculty of Science, Universiti Teknologi Malaysia, Skudai Johar Malaysia*

(Received 12 January 2012; revised manuscript received 12 March 2012)

Density functional theory based calculations have been carried out to study structural, electronic, and magnetic properties of $Zn_{1-x}Co_xO$ ($x = 0$, 0.25, 0.50, 0.75) in the zinc-blende phase, and the generalized gradient approximation proposed by Wu and Cohen has been used. Our calculated lattice constants decrease while the bulk moduli increase with the increase of Co^{2+} concentration. The calculated spin polarized band structures show the metallic behavior of Co-doped ZnO for both the up and the down spin cases with various doping concentrations. Moreover, the electron population is found to shift from the Zn–O bond to the Co–O bond with the increase of Co^{2+} concentration. The total magnetic moment, the interstitial magnetic moment, the valence and the conduction band edge spin splitting energies, and the exchange constants decrease, while the local magnetic moments of Zn, Co, O, the exchange spin splitting energies, and crystal field splitting energies increase with the increase of dopant concentration.

Keywords: density functional theory, magnetic semiconductors, generalized gradient approximation

PACS: 71.15.Mb, 71.15.Ap, 75.50.Pp, 71.20.Be **DOI:** 10.1088/1674-1056/21/9/097101

1. Introduction

Magnetic semiconductors are important for spintronic devices that exploit the charge and the spin degree freedoms of electrons for information processing and data storage.[1,2] The main challenge of these materials is the attainment of ferromagnetism having the Curie temperature comparable with or above room temperature and well-matching with the junction temperature.

Most of the ongoing researches focus on the wide band gap semiconductors and investigate the doping effect of transition metals (TMs) in search for the above room temperature ferromagnetism.[3] Being a II–VI compound semiconductor, ZnO with its direct and wide band gap has become one of the most promising host candidates for fabricating magnetic materials for room temperature applications. The ZnO based magnetic materials that show the ferromagnetic behaviors have motivated intensive research on structural and physical properties of these materials.[3,4,5−10]

Co-doped ZnO magnetic semiconductors are specially important in fabricating ferromagnetic devices.[11,12] The charge transfer in ZnO is because of the s and p electrons, while the magnetism in Co^{2+} is originated from its d electrons. Thus, the coupling between s, p and d electrons in Co-doped ZnO can be exploited for information processing and data storage. Moreover, the atomic radius of Co^{2+} (≈ 0.58 Å) is approximately equal to that of Zn (≈ 0.60 Å), and thus the solubility in ZnO is as high as 0.50% without disturbing the structural geometry.[13]

To the best of our knowledge, most of the theoretical and the experimental studies focused on the structural and the magnetic properties of the TM-doped ZnO in the wurtzite phase. Zhang *et al.*[17] have investigated the magnetic properties of Co^{2+} doped ZnO in the zinc-blende phase for the doping concentration of 12.5%. However, the above mentioned properties together with the electronic properties of the TM-doped ZnO in the zinc-blende phase have not been widely explored in theory and experiment.

In the present article, we study structural, electronic, and magnetic proprieties of the Co-doped ZnO in the zinc blende phase by using the density functional theory with the full potential linearized augmented plane wave (FP-LAPW) method at the gen-

*Project supported by the Ministry of Higher Education (MOHE) of Malaysia and the Universiti Teknologi Malaysia (UTM) (Grant Nos. Q.J13000.7126.00J33, R.J130000.7726.4D034, and R.J130000.7826.4F113.)

†Corresponding author. E-mail: rashidahmed@utm.my

© 2012 Chinese Physical Society and IOP Publishing Ltd

eralized gradient approximation (GGA) level. The calculations have been performed with the WIEN2k code. We organize the remaining paper as follows. In Section 2, the details of the computational method used are given. In Section 3, we discuss the calculated results for structural, electronic, and magnetic properties of $Zn_{1-x}Co_xO$ (x = 0, 0.25, 0.50, 0.75). The conclusion of our work is presented in Section 4.

2. Computational details

The density functional theory[14,15] calculation with the FP-LAPW and local orbital method[16,17] is one of the most accurate schemes for investigating the ground-state properties of materials. In this work, we used the WIEN2k code.[18] The generalized gradient approximation proposed by Wu and Cohen[19] has been used for the treatment of the exchange and the correlation potentials. ZnO in the zinc-blende phase has space group $F\bar{4}3m$ (No. 216) with lattice parameters $a = b = c = 4.60$ Å[20] and $\alpha = \beta = \gamma = 90°$. For $Zn_{1-x}Co_xO$ with $x = 0.25, 0.50, 0.75$, we used the B3 standard unit cell of $1 \times 1 \times 1$, which contained 8 atoms, and an appropriate number of Zn atoms were replaced by Co^{2+} to obtain the alloys. In our calculations, we chose the MT radii of Zn, Co^{2+}, and O to be 1.78 a.u., 1.78 a.u., and 1.58 a.u., respectively. The maximum value of the angular momentum was taken to be $l_{max} = 10$ for the expansion of the wave function inside the muffin tin sphere. In the interstitial region, the plane wave with cutoff parameter $K_{max} \times R_{MT} = 8$ was used for the wave function. For the Brillion zone integration, 70 k-points in the irreducible Brillion were used in our calculations. And we treated the $3d^{10}$, $4s^2$ electrons of Zn, the $3d^7$ electrons of Co, and the $2s^2$, $2p^4$ electrons of O as the valence electrons.

3. Results and discussion

3.1. Structural properties

The unit cells of $Zn_{1-x}Co_xO$ (x = 0, 0.25, 0.50, 0.75) are shown in Fig. 1. The conventional unit cell of ZnO in the zinc-blend phase contains 8 atoms with the space group of $F\bar{4}3m$ (No. 216) and atomic positions (0, 0, 0) for Zn and (1/4, 1/4, 1/4) for oxygen. In the zinc-blende phase, every atom is in a tetrahedral environment. We find that $Zn_{1-x}Co_xO$ with different doping concentration of Co has different space group. This is due to the small distortions in the structure caused by the doping of Co. For 25% and 75% doping concentrations of Co^{2+}, the alloys attain the space group of $P\bar{4}3m$ (No. 215). While the $Zn_{0.50}Co_{0.50}O$ alloy has the chalcopyrite type structure ($ZnCoO_2$) with space group $P\bar{4}m2$ (No. 115). For the study of structural properties of $Zn_{1-x}Co_xO$ (x = 0, 0.25, 0.50, 0.75), the volume of the super cell is optimized by using the Birch Murnaghan equation of state[21]

$$E(V) = E_0 - \frac{9V_0B_0}{16}\left\{\left[\left(\frac{V_0}{V}\right)^{2/3} - 1\right]^3 B_0' + \left[\left(\frac{V_0}{V}\right)^{2/3} - 1\right]^2\left[6 - 4\left(\frac{V_0}{V}\right)^{2/3}\right]\right\}, \quad (1)$$

where E_0 is the total energy, V_0 is the equilibrium unit cell volume, B_0 is the zero pressure bulk modulus, and B_0' is the pressure derivative of B_0.

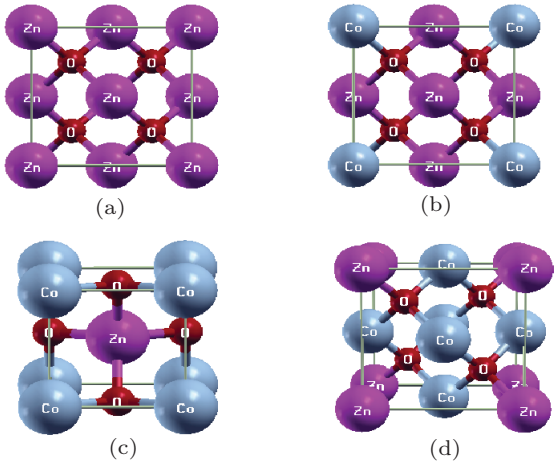


Fig. 1. (colour online) Unit cell structures of $Zn_{1-x}Co_xO$ with (a) x = 0, (b) x = 0.25, (c) x = 0.50, and (d) x = 0.75.

Our calculated results for V_0, lattice parameter a, and B_0 are listed in Table 1. From Table 1, it is clear that the substitution of Zn atoms by Co^{2+} affects the lattice constant and the bulk modulus of $Zn_{1-x}Co_xO$. The lattice constant a of $Zn_{1-x}Co_xO$ decreases linearly with the increase of the doping concentration of Co. This reduction in the lattice constant is due to the small mismatching of the atomic radii of Zn and Co. The change in the lattice constant also results in small distortions in the alloy. The bulk modulus of $Zn_{1-x}Co_xO$ increases with the increase of the Co^{2+} concentration or with the decrease of the lattice constant. The increase in the bulk modulus is linear for the doping concentrations studied (x = 0, 0.25, 0.50, 0.75). The increase in the bulk modulus reveals the increase in the hardness of the alloy, which indicates that $Zn_{0.25}Co_{0.75}O$ is the hardest.

Table 1. Calculated lattice constants of $Zn_{1-x}Co_xO$.

x	V_0/a.u.	a/Å	B_0/GPa
0	159.1763	4.55	146.2713
0[a)]		4.60	
0.25	632.3414	4.54	148.4343
0.5	312.4408	4.52	150.444
0.75	608.2593	4.48	152.9793

[a)] Experiment result from Ref. [14].

3.2. Electronic properties

3.2.1. Band structure

The band structure of ZnO is shown in Fig. 2(a). The energies of the conduction band (CB) and the valence band (VB) are arranged in such a way that the Fermi level lies at the zero energy represented by the dotted lines. For the undoped ZnO, the CB minima and the VB maxima lie at the same Γ point with an energy gap of 0.8 eV, which shows that the zinc-blende ZnO in its pure form exhibits a direct band gap. The band gap we calculated for ZnO is lower than the experimental value, but is in excellent agreement with the other theoretically calculated values.[22,23] The smaller value of our calculated band gap is because the GGA calculations always underestimate the band gap with respect to the experimental value. The second main reason for the obtained narrower band gap is that we do not consider the localization nature of d orbits in our calculations. The valence band of the undoped ZnO is mainly originated from O-2p and Zn-3d orbits, and the conduction band is mostly formed by the Zn-4s orbit. A strong hybridization between p and d orbits occurs, which pushes the 2p orbit of O very close to the 4s orbit of Zn and results in the narrowing of the band gap.

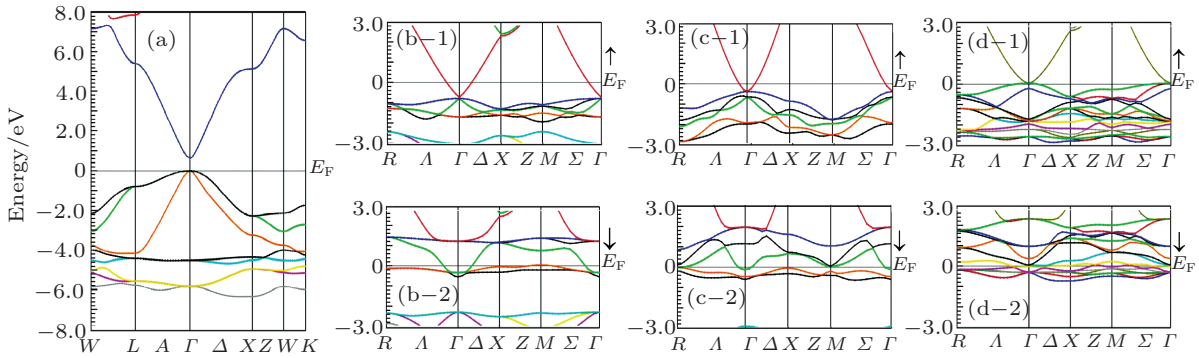


Fig. 2. (colour online) Band structures of $Zn_{1-x}Co_xO$ with (a) $x = 0$, (b) $x = 0.25$, (c) $x = 0.50$, and (d) $x = 0.75$. The up and the down arrows show the directions of spin. The Fermi level is located at 0 eV.

The band structures of $Zn_{1-x}Co_xO$ ($x = 0.25$, 0.50, 0.75) both for up and down spin configurations are shown in Fig. 2. Our calculated band structures for the ternary alloys are completely different from that for the binary compound ZnO. The semiconducting behavior of ZnO seems to disappear with the substitution of Co^{2+} over the entire doping range studied (0.25%, 0.50%, 0.75%). This may be due to the p–d hybridization between O-p and Co-d states,[24] or due to the underestimated band gap value in the GGA.

For $Zn_{0.75}Co_{0.25}O$ and $Zn_{0.50}Co_{0.50}O$, the spin polarized band structures shown in Figs. 2(b) and 2(c) indicate that for both up and down spin configurations, the CB minima overlap with the Fermi level at the Γ point. In the spin up band structure of $Zn_{0.75}Co_{0.25}O$, the VB maximum passes through the Fermi level and touches the CB minimum at the Γ point. We find a remarkable difference of electron population in the spin polarized band structures of $Zn_{1-x}Co_xO$ with $x = 0.25$, 0.50, 0.75. The down spin band is populated with more electrons than the up spin band. This difference in the up spin and the down spin bands results in the spontaneous magnetic moment, hence it indicates that $Zn_{1-x}Co_xO$ with $x = 0.25$, 0.50, 0.75 are ferromagnetic. The Co^{2+} atoms are responsible for the magnetization in these alloys. The CB of Co^{2+} contains the empty states of Co^{2+}, while the filled states appear inside the VB. In the up spin configuration, the Co^{2+} d states interact with the O p states. In the down spin configuration, the Co^{2+} states arise near the VB. The magnetism of the Co-doped ZnO is due to the interaction of delocalized Zn-4s states in CB and O-2p states in VB of ZnO with the localized partially filled d orbits of Co atoms,

which causes the strong hybridization between Co^{2+} 3d orbit and oxygen p orbit that shifts the up and the down spin orbits around the Fermi energy and results in the net magnetic moment.

3.2.2. Density of states

The spin polarized densities of states of $Zn_{1-x}Co_xO$ are arranged so that the spin up states are shown along the $+y$ axis and the spin down states are shown along the $-y$ axis. To check the magnetic behavior of the undoped ZnO, we perform the spin polarized calculations for it. The total and the partial densities of states for the up and the down spin configurations are shown in Fig. 3. In the figure, the up and the down spin states are shown to have a mirror symmetry, which reveals the equal numbers of up and down spin electrons in the unit cell of the undoped ZnO. Thus, no magnetic moment exists in the unit cell of the undoped ZnO. The unpolarized density of states (DOS) of ZnO is shown in Fig. 4. The VB of ZnO arises from the contribution of the Zn-3d states at lower energies together with the O-2p states appearing at the top of the VB. The CB is originated mainly from the Zn 4s states. A large dispersion of the d band with an energy width of 2.2 eV is shown in Fig. 4. This large dispersion of d band is due to the strong hybridization of p and d orbits in the VB that pushes the O-2p states closer to the CB and causes the band gap narrowing.

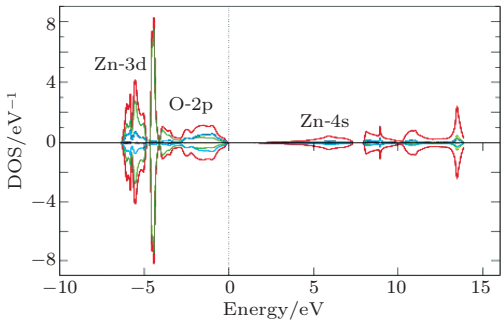


Fig. 3. (colour online) The spin polarized total and partial densities of states of ZnO. The up and the down spin states are shown in the positive and the negative sides of the plot, respectively. The Fermi level is located at 0 eV.

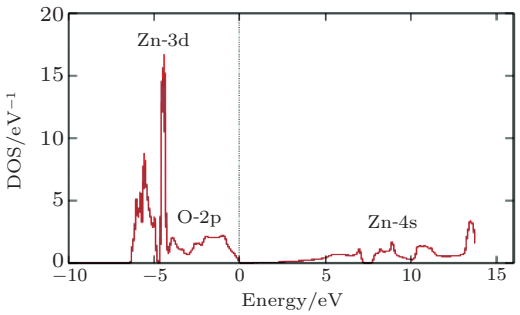


Fig. 4. (colour online) Total density of states of ZnO. The Fermi level is located at 0 eV.

The densities of state of $Zn_{1-x}Co_xO$ with $x = 0.25, 0.50, 0.75$ are shown in Figs. 5–7. The spin polarized densities of states of $Zn_{1-x}Co_xO$ are divided into three parts corresponding to the contributions of Zn, Co, and O. For $Zn_{0.75}Co_{0.25}O$, both the up and the down spin states with high densities in the energy range from −7.8 eV to −5 eV are formed by the Zn-3d states with a weak involvement of the 2p states of O and the 3d states of Co. For higher energies, the situation changes for the up and the down spin configurations. In the up spin configuration, states in the energy range from −5 eV to −2.6 eV are usually from the 2p states of O and the 3d states of Co. The upper states of the VB, which are further divided into two groups in the energy range from −2 eV to −0.85 eV, arise mostly from the Co d states that contain e_g and and t_{2g} with an energy width of 1.15 eV. In the spin down configuration, states in the energy range from −5 eV to −2.5 eV of the VB are formed by the O-2p orbit. The peak appearing in the range from −0.25 eV to near the Fermi energy E_F arises due to the Co-3d states. In the up spin configuration, the conduction band minimum is dominated by the Zn-4s states, while in the down spin configuration, the conduction band minimum is mainly from the Co-3d states. In the spin up configuration, with the increase of Co concentration in $Zn_{1-x}Co_xO$, the O-2p states in the VB become more broaden due to the interaction with the d states of Co. This p–d interaction pushes the VB

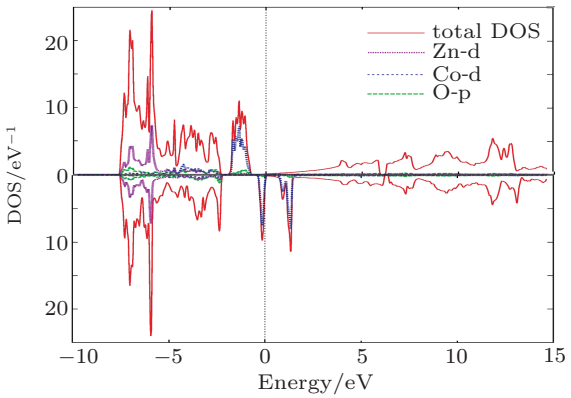


Fig. 5. (colour online) The spin polarized total and partial densities of states of $Zn_{0.75}Co_{0.25}O$. The up and the down spin states are shown in the positive and the negative sides of the plot, respectively. The Fermi level is located at 0 eV.

maximum towards the Fermi energy. The metallic behavior of the Co-doped ZnO is essentially caused by the strong interaction of O-2p and Co-3d states, while the ferromagnetism observed in the Co-doped ZnO is originated from the p–d interaction. Moreover, the total densities of up and down spin electrons are obviously split in the vicinity of the Fermi level, which indicates that the spin arrangement is dominated by the exchange interaction.

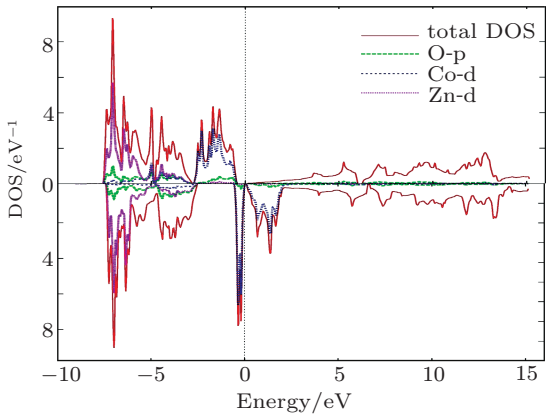


Fig. 6. (colour online) Total and partial density of states of $Zn_{0.50}Co_{0.50}O$. The up and the down spin states are shown in the positive and the negative sides of the plot, respectively. The Fermi level is located at 0 eV.

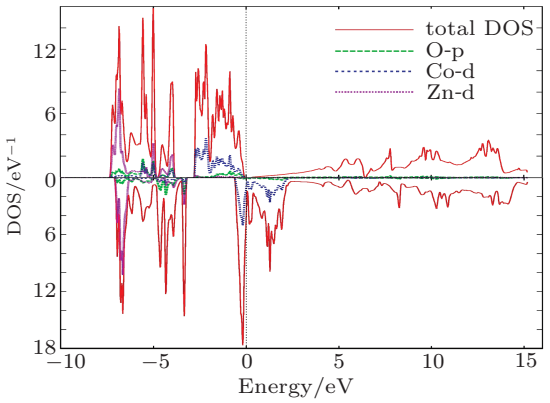


Fig. 7. (colour online) Total and partial densities of states of $Zn_{0.25}Co_{0.75}O$. The up and the down spin states are shown in the positive and the negative sides of the plot, respectively. The Fermi level is located at 0 eV.

In the zinc-blende phase, Co^{2+} has a tetrahedral environment, each Co^{2+} ion is surrounded by four oxygen atoms. The crystal field splitting effect occurs due to these O atoms, the Co five-fold d-state degeneracy is lifted, the states are split to two groups of states, the lower energy doublet states e_g and the higher energy triplet states t_{2g}. As a consequence of the large spin exchange splitting, the full occupation of the e_g states is expected,[25] while the t_{2g} down spin states are half filled. The electronic configuration of the occupied states in the zinc-blende phase is $(e_g^{\uparrow})^2(t_{2g}^{\uparrow})^3(e_g^{\downarrow})^2$, which leads to a magnetic moment close to $3\mu_B$ per Co atom. For $Zn_{0.75}Co_{0.25}O$, the e_g and the t_{2g} states are found to be centered at energies -2.84 eV and -2.25 eV respectively in the up spin case, while in the down spin case, these states are at -0.157 eV and 1.2827 eV, respectively. For $Zn_{0.50}Co_{0.50}O$, in the up spin case, the corresponding energies are -2.35 eV and -1.7576 eV, in the down spin case, they are 1.3 eV and 0.254 eV, respectively. For $Zn_{0.25}Co_{0.75}O$, in the up spin case, the states are correspondingly centered at -2.21 eV and -1.6 eV, while in the down spin case,they are centered at -0.3 eV and 1.3 eV, respectively.

3.2.3. Charge density

The charge density is an important tool to visualize the bond nature, the bonding properties, and the charge transfer. The ground-state charge density of ZnO in the zinc-blende phase obtained in our calculations is shown in Fig. 8. The total charge density has been plotted in the (110) plane. Figure 8 shows that the Zn atom has more core electrons populated near the nucleus, thus the charge density in the vicinity of the nucleus is higher. While the oxygen atom has a large number of valence electrons, and the charge density is more spread out than that of Zn. The large difference of electronegativity between Zn and O results in the difference of charge transfer.

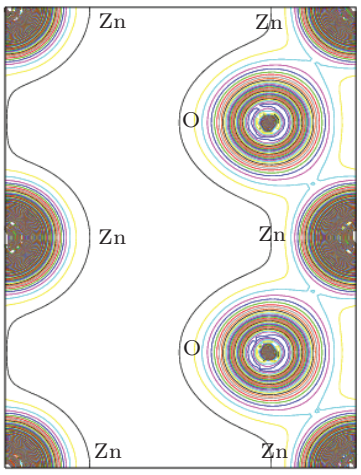
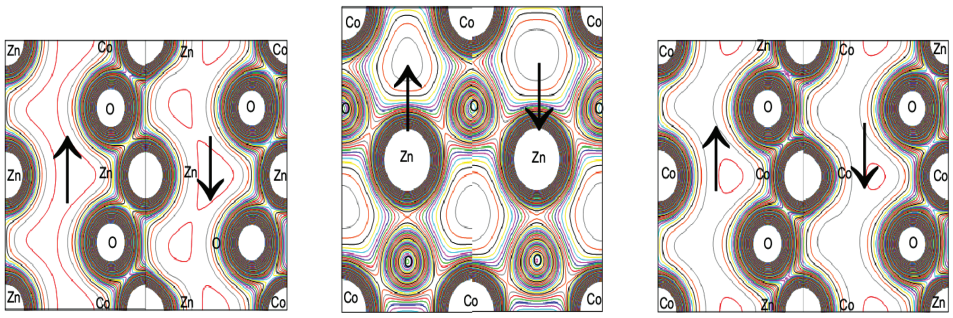


Fig. 8. (colour online) The contour plot of total valence charge density in the (110) plane for ZnO in the zinc-blende phase.

The difference in the charge transfer between anion and cation is directly proportional to the dissimilarity in the electronegativity. The contour plot of charge density shown in Fig. 8 reveals that the Zn–O bond is covalent with strong ionic behavior. Moreover, the electrons are accumulated along the Zn–O bond and are deflected to the oxygen atom.

The contour plot for the charge density of $Zn_{0.75}Co_{0.25}O$ shown in Fig. 9(a) indicates the accumulations of electrons along the Zn–O and the Co–O bonds. In $Zn_{0.75}Co_{0.25}O$, the O atoms are covalently bonded with both Zn and Co atoms, and the population of electrons in the Zn–O bond is more than that in the Co–O bond. The electrons population is greater in the spin down case than that in the spin up case. The charge density contour plot of $Zn_{0.50}Co_{0.50}O$ shown in Fig. 9(b) indicates that the populations of electrons in the Zn–O and the Co–O bonds are approximately equal to each other. In $Zn_{0.50}Co_{0.50}O$, the populations of electrons in the up and the down spin configurations remain almost equal. The spin polarized charge density contour plot of $Zn_{0.25}Co_{0.75}O$ is shown in Fig. 9(c). The figure shows that approximately the same number of electrons appear in the Zn–O and the Co–O bonds in the up spin case, while in the down spin case, the Co–O bond is more populated with electrons than the Zn–O bond.



(a) (b) (c)

Fig. 9. (colour online) The spin polarized contour plots of total valence charge density in the (110) plane for $Zn_{1-x}Co_xO$ with (a) $x = 0$, (b) $x = 0.25$, (c) $x = 0.50$, and (d) $x = 0.75$ in the zinc-blende phase.

4. Magnetic properties

We also calculate the total and the local magnetic moments of $Zn_{1-x}Co_xO$ (x = 0, 0.25, 0.50, 0.75), as shown in Table 2. The observed magnetic moments in these alloys are originated from the Co-3d states. Table 2 reveals that the total magnetic moment of $Zn_{1-x}Co_xO$ decreases with the increase of the doping concentration of Co^{2+}.

Table 2. Calculated parameters of $Zn_{1-x}Co_xO$.

	ZnO	$Zn_{0.75}Co_{0.25}O$	$Zn_{0.50}Co_{0.50}O$	$Zn_{0.25}Co_{0.75}O$
M^{Total}	0.00012	3.02232	3.00006	2.98934
M^{Co}	–	2.35711	2.36168	2.39763
M^{Zn}	0.00042	0.01354	0.02865	0.04594
M^{O}	0.00040	0.08123	0.16442	0.27479
M^{Inter}	0.00070	0.29967	0.28091	0.21001
ΔE_{c}	0	0.37	0.21	–0.233
ΔE_{v}	0	0.42	-0.01	–0.413
Δ_X(d)	–	3.10029	3.73734	3.96929
$\Delta E^{\uparrow}_{\mathrm{cry}}$	–	0.59	0.592	0.61
$\Delta E^{\downarrow}_{\mathrm{cry}}$	–	1.439	1.554	1.60
N_α	0	1.25577	0.3556	–0.259
N_β	0	1.4254	–0.01693	-0.4593

Our calculations for $Zn_{1-x}Co_xO$ are performed in the zinc-blende phase, but according to Ref. [26], the structure cannot be exactly the same as that of ZnO, some doping Co atoms would be accommodated at the interstitial sites. These Co interstitial atoms together with the Zn and the substitutional Co atoms and the anti-site O atoms are responsible for the net magnetic moment observed in $Zn_{1-x}Co_xO$. From Table 2, it is clear that the local magnetic moment of Co in $Zn_{1-x}Co_xO$ is smaller than its corresponding value in free space $3\mu_B$. This decrease in the local magnetic moment of Co is attributed to the the p–d hybridization. By increasing the Co concentration, the substitutional Co magnetic moment is increased. This increase is because of the decrease in the interstitial Co magnetic moment. The net magnetic moment of the corresponding alloy is found to be smaller than the sum of their individual values, as shown in Table 2. This discrepancy in the net magnetic moment and the sum of their individual values is because of the negative p–d interaction between Co-3d and O-2p orbits that decreases the total energy.

We calculate the spin exchange splitting $\Delta_X(\mathrm{d})$ for $Zn_{1-x}Co_xO$, which determines the separation between the up and the down spin d-state maximum intensities and can be represented by $\Delta_X(\mathrm{d}) = E(C_\mathrm{d}^\downarrow) - E(C_\mathrm{d}^\uparrow)$. The calculated values for $\Delta_X(\mathrm{d})$ are listed in Table 2. Table 2 shows that with the increase of the doping concentration of Co, $\Delta_X(\mathrm{d})$ decreases. We can also correlate $\Delta_X(\mathrm{d})$ with the magnetic moment, i.e., $\Delta_X(\mathrm{d})$ decreases with the decrease of the magnetic moment. The calculated spin polarized crystal field splitting ΔE_cry in $Zn_{1-x}Co_xO$ is listed in Table 2. The ΔE_cry increases with the increase of the Co concentration in $Zn_{1-x}Co_xO$. From Table 2, we note an inverse relation between ΔE_cry and the total magnetic moment M, i.e., ΔE_cry increases with the decrease of M. The ΔE_cry is found to be smaller than spin exchange splitting $\Delta_X(\mathrm{d})$ for each value of doping concentration. This results in the approximately full filled e_g states and the half filled spin down t_{2g} states.

Moreover, we calculate the exchange constants N_α and N_β for the conduction and the valence bands using the relations[27−29]

$$N_\alpha = \frac{\Delta E_\mathrm{c}}{x\langle S\rangle}, \tag{2}$$

$$N_\beta = \frac{\Delta E_\mathrm{v}}{x\langle S\rangle}, \tag{3}$$

where $\Delta E_\mathrm{c} = E_\mathrm{CBmin}^\downarrow - E_\mathrm{CBmin}^\uparrow$, $\Delta E_v = E_\mathrm{VBmax}^\downarrow - E_\mathrm{VBmax}^\uparrow$, $\langle S\rangle$ is the half magnetic moment of the Co^{2+} ion, and x is the doping concentration. The calculated values of ΔE_c, ΔE_v, N_α, and N_β are listed in Table 2, where the magnetic moments and the energies are in units of μ_B and eV, respectively. It is clear that N_α and N_β decrease with the increasing x.

To the best of our knowledge, the valence and the conduction band edge spin splitting energies, the crystal field splitting energies, the exchange spin splitting energies, and the exchange constants for Co doped ZnO are provided here for the first time and can be used as a reference.

5. Conclusion

We have studied structural, electronic, and magnetic properties of $Zn_{1-x}Co_xO$ with $x = 0$, 0.25, 0.50, 0.75 in the zinc-blende phase by using the full potential linearized augmented plane wave method at the generalized gradient approximation level within the density functional theory (DFT). The results obtained show that the lattice constants decrease and the bulk moduli increase with the increase of the Co concentration. The GGA calculations for the electronic properties reveal that the band structure and the density of states of the Co-doped ZnO are changed significantly in comparison with those of the pure ZnO, and reveal the metallic behavior for both up and down spin configurations. The magnetic moment observed mainly arises from the interaction between the O-p and the Co-d states. The total magnetic moment, the interstitial magnetic moment, the valence and the conduction band edge spin splitting energies, and the exchange constants are found to decrease, while the local magnetic moments of Zn, Co, and O, the exchange spin splitting energies, and the crystal field splitting energies increase linearly with the increase of the Co concentration.

References

[1] Ohno H 1998 *Science* **281** 951

[2] Wolf S A, Awschalom D D, Buhman R A, Daughtin J M, Molnar S V, Roues M L, Chtchelkanova A Y and Treger D M 2001 *Science* **294** 1488

[3] Dietl T, Ohno H, Msatsukura F, Cibert J and Ferrand D 2000 *Science* **287** 1019

[4] Sato K and Yoshida H K 2000 *Jpn. J. Appl. Phys.* **39** L555

[5] Hu S J, Yan S S, Zhao M W and Mei L M 2006 *Phys. Rev.* B **73** 245205

[6] Fritsch D, Schmidt H and Grundmann M 2006 *Appl. Phys. Lett.* **88** 134104

[7] Venkatesan M, Fitzgerald C B, Lunney J G and Coey J M 2004 *Phys. Rev. Lett.* **93** 177206

[8] Liu C, Yun F, Morkoc H and Mater J 2005 *Science* **16** 555

[9] Yan W, Sun Z, Liu Q, Zhongrui L, Shi T, Wang F, Qi Z, Zhang G, Wei S, Zhang H and Chen Z 2007 *Appl. Phys. Lett.* **90** 242509

[10] Brihi N, Takkouk Z and Bouaine A 2007 *Mater. Sci. Eng.* B **14** 6

[11] Belghazi Y, Schmerber G, Colis S, Rehspringer J L, Berrada A and Dinia A 2007 *J. Magn. Mater.* **310** 2092

[12] Ueda K, Tabata H and Kawai T 2001 *Appl. Phys. Lett.* **79** 988

[13] Zhang J, Yao K L, Liu Z L and Gao G Y 2010 *Physica* B **405** 1447

[14] Hohenberg P and Kohn W 1964 *Phys. Rev.* B **864** 136

[15] Kohn W and Sham L S 1965 *Phys. Rev.* **140** 1133

[16] Sjstedt E, Nordstrm L and Singh D J 2000 *Solid State Commun.* **114** 15

[17] Schwarz K, Blaha P and Madsen G K H 2002 *Comput. Phys. Commun.* **147** 71

[18] Blaha P, Schwarz K, Madsen G K H, Kvasnicka D and Luitz J 2001 *WIEN2K* (Vienna: Techn. Universitat)

[19] Wu Z and Cohen R E 2006 *Phys. Rev.* B **73** 235116

[20] Jaffe J E and Hess A C 1993 *Phys. Rev.* B **48** 7903

[21] Brich F 1952 *J. Geophys. Res.* **57** 227

[22] Benam M R, Hezari M and Shayan F 2011 *International Journal of the Physical Sciences* **6** 1112

[23] Palacios P, Aguilera I and Wahnn P 2010 *Thin Solid Films* **518** 4568

[24] Rozale H, Lakdja A, Lazreg A and Ruterana P 2010 *Phys. Status Solidi* B **247** 1641

[25] Walsh A, Da Silva J L F and Wei S H 2008 *Phys. Rev. Lett.* **100** 256401

[26] Masek J, Kudrnovsky J and Maca F 2003 *Phys. Rev.* B **67** 153203

[27] Sanvito S, Ordejon P and Hill N A 2001 *Phys. Rev.* B **63** 165206

[28] Echeverria-Arrondo C, Perez-Conde J and Ayuela A 2010 *Phys. Rev.* B **82** 205419

[29] Raebiger H, Ayuela A and Nieminen R M 2004 *J. Phys.*: *Condens. Matter* **16** 457